The Separation of Cell Suspensions Isolated from Coelomic Fluid and Coelomic Epithelium of the Starfish *Asterias rubens* in Percoll Density Gradients

Natalia Sharlaimova, Sergey Shabelnikov, Dan Bobkov and Olga Petukhova

Abstract: The regeneration process assumes the presence in the body of cells capable of self-renewal and subsequent differentiation into specialized cells. Whether these cells are stem cells or are present in circulating fluids or tissues as a pool of reserve progenitor cells, or whether they appear following dedifferentiation/transdifferentiation of specialized cells of individual tissues, are the main questions that scientists are focusing on. Understanding the origin and pathways of differentiation in coelomic fluid cells and coelomocytes of the starfish *Asterias rubens* was the aim of this research. The coelomic epithelium is considered as a possible source of coelomocytes. Further effective studies of coelomocyte replenishment are difficult due to the lack of protein markers characterizing various cell morphotypes. Additional difficulties lie in the heterogeneity of analyzed cell populations. In the present study, we separated cells of the coelomic fluid and the coelomic epithelium, and a subpopulation of the coelomic epithelium enriched with poorly differentiated cells, which are proposed precursors of some types of coelomocytes, in a Percoll density gradient. Characterization of the cell morphology of different fractions and their behavior in vitro (functional characteristics) revealed an enrichment of the gradient fractions in two of eight types of coelomocytes and three of eight morphotypes of cells of the coelomic epithelium.

1. Introduction

The origin of cells contributing to tissue homeostasis and regeneration is one of the fundamental questions of biology (Rinkevich et al. 2022). Typical examples of adult invertebrate stem cells include sponge archaeocytes and choanocytes (Simpson 1984; Funayama 2018), cnidarian interstitial cells (Bosch 2009), flatworm neoblasts (De Mulder et al. 2009; Rossi and Salvetti 2019), and annelid teloblasts (Sugio et al. 2012).

Deuterostome invertebrates provide a significant pool of results supporting the hypothesis of the dominant role of dedifferentiation or transdifferentiation of body cells as the main mechanisms of regeneration, while the participation of stem cells has been proven to tunicate hemoblasts (Ferrario et al. 2020; Kassmer et al. 2020). Studying the origin and fate of individual cells will answer many questions

related to elucidating the mechanisms of tissue renewal. A prerequisite for this is the characterization of molecular markers of specialized and undifferentiated cells.

The coelomocyte replenishment of the starfish *Asterias rubens* is an example of maintenance of tissue homeostasis (Pellettieri and Alvarado 2007; Blanpain and Fuchs 2014). Coelomocytes are a heterogeneous cell population of the main body cavity of a starfish, or the coelom. Coelomocytes are responsible for various functions including immune defense, nutrient transport, and formation of aggregates in the zones of body damage (clotting reaction) (Smith 1981; Dogel 1981; Chia and Xing 1996). The coelomic cavity and organs located in it are lined with a ciliated epithelium, called the coelomic epithelium (CE) (Dogel 1981; Blowes et al. 2017).

The concept of the origin of mature coelomocytes from the CE of the starfish *A. rubens* is based on the work of French authors (Bossche and Jangoux 1976). Our own data showed the presence of a significant pool of cells on the surface of the CE, including small poorly differentiated cells named small epithelial cells of type 1 (SECs-1) (Sharlaimova et al. 2014, 2020). SECs-1 comprise about 50% of an individual subpopulation of weakly attached CE cells (CE-W), which can be collected and analyzed separately (Sharlaimova et al. 2014, 2020). Indirect data (experiments with a conditionally intact epithelium) of the same work suggested cell migration from the epithelium. Moreover, morphological analysis suggests that these cells may be precursors of coelomocytes (Sharlaimova and Petukhova 2012).

The question of the origin of SECs-1 on the surface of the CE remains unclear. It could be due to the activity of stem cells that serve as a pool of reserve cells, or it could result from dedifferentiation of specialized cells, for example, ciliated cells of the CE (Bossche and Jangoux 1976) or myoepithelial cells (García-Arrarás and Dolmatov 2010). Further effective studies answering this question are difficult due to the lack of protein markers characterizing various cell populations. To track the fate of cells, it is necessary to identify molecular markers for different types of cells, both undifferentiated and specialized.

The heterogeneity of cell populations is an additional problem for the search for markers of certain types of cells, since the concentration of marker proteins specific for a certain type of cell decreases in the mixture of cells, which leads to a decrease in the efficiency of mass spectrum analysis.

The dominant types of cells in the coelomic fluid (CF) of *A. rubens* identified after azure-eosin staining were small and large petaloid agranulocytes. A homogeneous substance characterized the cytoplasmic matrix of these cells. Eosinophilic granulocytes, roundish agranulocytes, fusiform cells, two types of small cells with a high nuclear–cytoplasmic ratio, and bi- or trinucleated cells were less represented among coelomocytes (Sharlaimova et al. 2020).

Mass spectrometric analysis, performed in our previous work (Sharlaimova et al. 2020), identified only two proteins (integrin alpha 8 and integrin beta 1) that

could serve as markers in a cell differentiation study among the proteins in the total coelomocyte suspensions.

The dominant cell type of the CE (30%) is represented by small agranulocytes. A significant part of small agranulocytes, possessing irregularly shaped nuclei and tending to form aggregates, was identified as ciliated epithelial cells after alpha-tubulin staining (Sharlaimova et al. 2014, 2020). Other cell types included large agranulocytes, small azurophilic granulocytes, large eosinophilic granulocytes, morula cells, myoepithelial cells, and two types of small cells with a high nuclear–cytoplasmic ratio (Sharlaimova et al. 2014). Unique CE proteins identified in the total cell suspensions were represented (according to Gene Ontology analysis) by oxidoreductase activities only, although visual inspection revealed one regulatory protein unique to this population (ninjurin) (Sharlaimova et al. 2020). However, several proteins involved in the regulation of proliferation and differentiation processes were identified in a subpopulation of weakly attached CE cells (CE-W), which can be collected and analyzed separately (Sharlaimova et al. 2014). The CE-W cell subpopulation is 50% enriched with small cells with a high nuclear–cytoplasmic ratio (SECs-1). Importantly, SECs-1 demonstrate proliferative activity in vivo and in vitro. They were proposed as precursors of some coelomocyte types (Sharlaimova and Petukhova 2012).

One of the approaches to solving the problem of heterogeneous cell suspension analysis is the preliminary fractionation of cells in density gradients to obtain fractions enriched in specialized morphotypes. Examples of successful separation of invertebrate cells have been reported in the literature (Kudryavtsev et al. 2016; Lin et al. 2001; Kauschke et al. 2001; Hamed et al. 2005).

The aim of this study was the separation of CF and CE cell suspensions by Percoll density gradient centrifugation, and the characterization of cell fractions by histological and immunofluorescent staining and by functional tests in vitro. Morphological and functional analysis of cells of different CF and CE fractions showed that cell separation in the Percoll density gradients allows obtaining fractions of CF and CE cells enriched with certain morphotypes.

Morphological and functional analysis of CF cells showed the enrichment of fraction 1 with roundish coelomocytes unable to form networks (a characteristic property of coelomocytes) and fraction 4 circulatory coelomocytes with petaloid agranulocytes that form networks in vitro. For CE cells, enrichment with ciliated cells in fractions 3 and 4 and enrichment with small epithelial cells of the second type (SEC-2), another type of proliferating CE cell (Sharlaimova et al. 2014), in fractions 1 and 2 were found. For CE-W cells, additional enrichment with SECs-1 in fractions 1–3 was obtained.

2. Materials and Methods

2.1. Animal Manipulation

Experiments were performed at the Biological Station of the Zoological Institute, Russian Academy of Sciences, on Cape Kartesh (Kandalaksha Bay, the White Sea), in September 2018–2020. Intact *A. rubens* L. (Asteroidea, Echinodermata) specimens, 10–15 cm in diameter, were collected off Fettakh Island and kept in cages at a depth of 3–5 m throughout the experimental period. They were fed ad libitum with a diet of mussels. Some experiments were also carried out on animals deprived of food for 4 days.

2.2. Isolation of Circulatory Coelomocytes

The CF was collected after cutting off an arm tip and filtering the fluid through a nylon gauze (70 mesh) into a test tube with saline solution free of Ca^{2+} and Mg^{2+} (CMFSS, Kanungo 1982) and then supplemented with 15 mM EDTA (anticoagulant buffer) (Sharlaimova et al. 2020). The cells were pelleted by centrifugation at 550× *g* for 10 min and washed twice in CMFSS. About 200 × 10^6 circulatory coelomocytes could be isolated from 4 freshly caught starfish with a diameter of 10–15 cm.

2.3. Isolation of Coelomic Epithelium Cells (Epitheliocytes)

Fragments of the CE were detached with forceps from the inner surface of the aboral body wall of the arm and washed with CMFSS. The washing solution obtained at this step contained a considerable number of cells, which were classified as an individual subpopulation of weakly attached CE cells (CE-W) (Sharlaimova et al. 2014, 2020). They were collected and analyzed separately. Remaining CE fragments were treated with 0.05%–0.1% crab hepatopancreas collagenase (Biolot, Russia) in CMFSS for 15 min with periodic pipetting to obtain the dissociated cells. The CE-W cell preparation and dissociated CE cells were filtered through a nylon gauze, pelleted from the suspension by centrifugation at 550× *g* for 10 min, and washed twice with CMFSS. About 500 × 10^6 CE cells and 100 × 10^6 CE-W cells could be isolated from 4 freshly caught starfish with a diameter of 10–15 cm.

2.4. Cell Separation in Discontinuous (Step) Percoll Density Gradients

CF and CE cell separation was performed in discontinuous (steps 50%–45%–40%–35%–30%–25%, 1 mL each) Percoll density gradients using the

Amersham protocol with modification (Percoll Methodology and Applications Amersham Biosciences[1]).

CF and CE cell separation was performed in discontinuous (steps 50%–45%–40%–35%–30%–25%, 1 mL each) Percoll density gradients using the manufactory protocol (GE Healthcare, Sweden, Uppsala) with modification.

To prepare a stock isotonic Percoll (SIP) solution, 9 parts (v/v) of Percoll were added to 1 part (v/v) of 10× CMFSS solution. To form Percoll density gradients, SIP was diluted to lower densities by adding CMFSS and then layered in 15 mL polycarbonate centrifuge tubes (Sarstedt, Germany), starting with the densest at the bottom of the tube using a 3 mL syringe fitted with a 21 G needle.

The coelomocyte suspension was layered on top in 0.5 mL of CMFSS/5 mM EDTA (about 33 × 10^6 per gradient), and tubes were centrifuged at 400× *g* for 20 min at 8 °C using a swing-out bucket. CE and CE-W cell suspensions were layered in 0.5 mL of CMFSS (about 70 × 10^6 CE cells per gradient and 90–110 × 10^6 CE-W cells per gradient), and tubes were centrifuged at 400× *g* for 20 min at 8 °C using a swing-out bucket.

The visible layers of cells at phase boundaries were collected with a Pasteur pipette, transferred into the tubes with 7 mL CMFSS, and then centrifugated at 550× *g* for 10 min at 8 °C. Cells were resuspended in 1 mL of CMFSS, the number of cells in each fraction was counted with a hemocytometer, and cell suspensions were subdivided for fixation and functional tests. The number of cells in all fractions was summed up, and the proportion of cells in each fraction was calculated (%).

2.5. Histological and Immunofluorescent Staining of CF and CE Cell Suspensions

The circulatory cells of the CF, and CE and CE-W cells were fixed with 4% paraformaldehyde (PFA), placed onto coverslips coated with poly-L-lysine (Sigma) (0.5–1.0 × 10^6 cells), and stained with azure-eosin or DAPI. Preparations were examined in transmitted light or in fluorescence light at a ×100 objective lens magnification under an Axiovert 200M microscope (Carl Zeiss, Jena, Germany) fitted with a Leica DFC420 digital camera.

The efficiency of cell fractionation in Percoll density gradients was estimated by comparing the proportion of distinct cell morphotypes, identified after staining the nuclei with DAPI under an Axiovert 200M microscope (Carl Zeiss, Germany), in each gradient fraction. In order to use the previously proposed terminology to characterize cell morphotypes (Sharlaimova et al. 2014, 2020), we compared the morphotypes of cells after staining with azure-eosin and DAPI. The criteria were cell and nucleus size and shape, presence or absence of granules, and the pattern

[1] Available online: www.amershambiosciences.com (accessed on 23 July 2021).

and intensity of staining. Cell sizes were determined from images obtained with a camera with a known resolution. Cell counts in three parallel samples were taken in several randomly selected microscopic fields (in total, no less than 400 cells were analyzed in each sample).

2.6. Functional Test of Cell Fractions In Vitro

For the functional test, cells of individual fractions were washed in CMFSS, precipitated by centrifugation at 550× *g* for 10 min, resuspended in sterile seawater, and plated onto 96-well plates in a volume of 100 µL (0.5×10^6 of CF cells, and 0.8×10^6 of CE and CE-W cells per well). The samples were photographed in transmitted light with an inverted Biolam microscope at different intervals of incubation in seawater: 1.5 and 18 h for coelomocytes, and 18 h for CE cells. For detecting ciliated CE cells, cells from Percoll density gradient fractions were placed onto the coverslips for 18 h, fixed with 4% PFA, permeabilized with 0.1% Triton X-100, and stained with anti-tubulin antibodies, 1:1500 (Sigma, New York, NY, USA), and DAPI (Sigma, USA). Preparations were examined at a ×63 objective lens magnification under a Leica TSC SP5 confocal microscope (Leica Microsystems, Wetzlar, Germany).

2.7. Statistics

The data of CF and CE cell population compositions are expressed as mean ± SEM ($p < 0.05$); the data concerning the proportion of cells in different fractions are expressed as box and whisker plots with the designation of means, SE, SD, and outliers. All data were processed statistically by ANOVA with Tukey's HSD multiple comparison test to determine significant differences ($p < 0.05$), using the STATISTICA 7.0 Software.

3. Results

3.1. Separation of Cell Suspensions in Percoll Density Gradients

Separation of CF cells and CE cells in Percoll density gradients was carried out for cell suspensions isolated from animals kept in cages.

Separation of both coelomocytes and CE cell suspensions in a six-step gradient led to the concentration of cells in six zones: at the border of 25%—fraction 1; at the border of 25%–30%—fraction 2; at the border of 30%–35%—fraction 3; at the border of 35%–40%—fraction 4; at the border of 40%–45%—fraction 5; and at the border of 45%–50%—fraction 6 (Figure 1A). Preliminary experiments showed that fraction 6 of coelomocytes and the CE contained an insignificant proportion of cells (<0.5%), and they were represented, to a large extent, by cells with fragmented nuclei. Therefore, no further analysis of this fraction was carried out.

3.2. Coelomocyte Separation in Percoll Density Gradients

3.2.1. Composition of Gradient Fractions

The relative proportion of the total cells across the different fractions varied in different experiments. The fact of significant variability in the number of cells in fractions 1 and 4–5 was confirmed by statistical analysis (n = 12), showing the maximal variation in cell number in these fractions (Figure 1B).

The efficiency of cell separation in gradients was assessed by comparing the composition of cell fractions with the composition of the total cell suspension. Images were obtained, using a combination of immunofluorescence and bright-field light microscopy, after staining the nuclei with DAPI (Figure 1C). The cell size was determined at the light optical level after the attachment of the fixed cells to the coverslips coated with poly-L-lysine. The cells corresponding to them in morphology, revealed in CF previously after staining of cell suspensions with azure-eosin, are shown next to each type (Figure 1C).

These cells comprise eight morphotypes: small coelomocytes (4.4 $\pm$ 0.25 μm) with a high nuclear–cytoplasmic ratio, having discretely (Figure 1C(a)) or densely (Figure 1C(b)) stained nuclei and invisible cytoplasm; petaloid agranulocytes of small (7.33 $\pm$ 0.2 μm) and large (11.7 $\pm$ 0.7 μm) sizes with densely stained nuclei (Figure 1C(c,d), respectively); roundish agranulocytes with densely stained nuclei (8.2 $\pm$ 0.46 μm) (Figure 1C(e)); eosinophilic granulocytes with weakly stained nuclei (10.84 $\pm$ 0.28 μm) (Figure 1C(f)); bi- or trinucleated cells with densely stained nuclei (12.4 $\pm$ 0.5 μm) (Figure 1C(g)); and fusiform cells (15 $\pm$ 0.5 μm) (Figure 1C(h)). In the calculations presented in Figure 1C(a,b), small coelomocytes with a high nuclear–cytoplasmic ratio or discretely or densely stained nuclei were combined into one type due to their insignificant proportion. Enrichment for these types of cells was found in fraction 3. Moreover, fusiform cells were combined with the class of large agranulocytes due to their insignificant proportion (less than 1% in each field of view).

The data analysis showed that fractions 1 and 2 were enriched (58% and 41%, respectively) with roundish (not petaloid) agranulocytes mainly with fine-grained or smooth cytoplasm (Figure 1C(e)). These cells in the total suspension make up an insignificant fraction. Azure-eosin staining showed that roundish cells possessed densely stained nuclei, unlike weakly stained nuclei of eosinophilic granulocytes, and there were no granules detected (Figure 1C(e)). Therefore, it is unlikely that they are granulocytes. Most of the large petaloid agranulocytes are distributed between fractions 3 and 5, while in fractions 1–2, their share is significantly reduced (up to 15% in fraction 1).

Granulocytes and two nuclear cells were more abundant in fraction 5 (35% and 5%, respectively) (Figure 1C(f,g)).

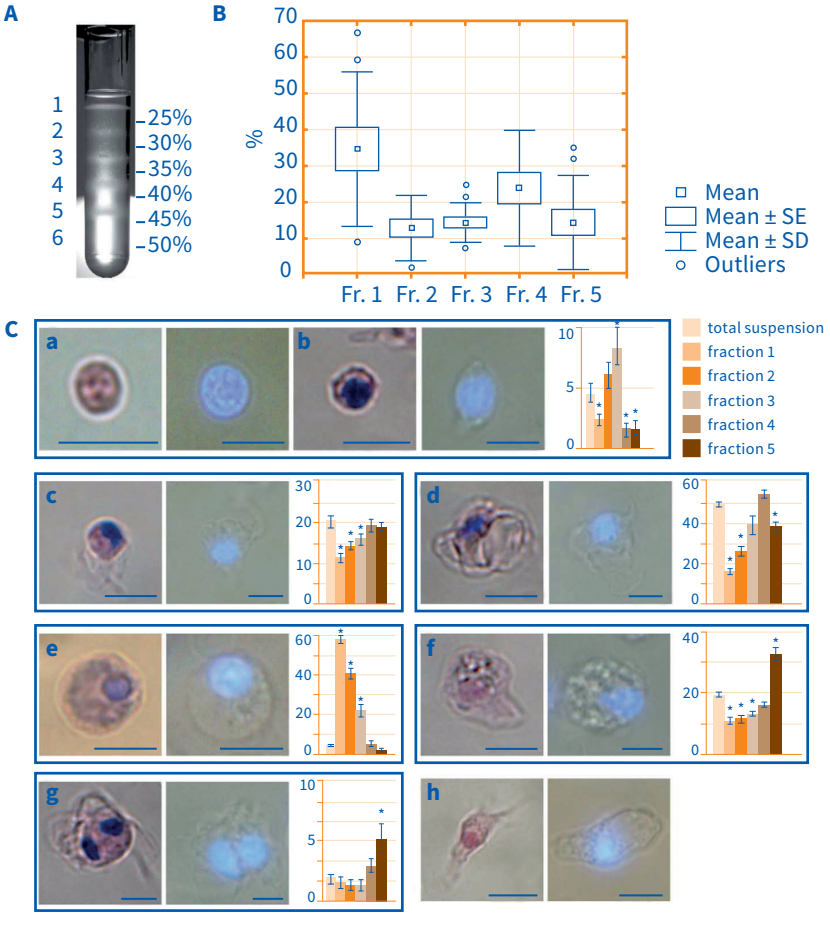

Figure 1. Coelomocyte separation in discontinuous Percoll density gradients. (**A**) An example of *Asterias rubens* coelomocyte separation using six-step Percoll density gradients, (**B**) the portion of cells in different fractions, and (**C**) the coelomocyte types revealed after azure-eosin staining and staining of cell suspensions with DAPI, and the proportion of this type in each gradient fraction: (**a**) small coelomocyte with discretely stained nuclei and invisible cytoplasm; (**b**) small coelomocyte with densely stained nuclei and invisible cytoplasm (data for types (**a**,**b**) were combined); (**c**) small petaloid agranulocyte with densely stained nuclei; (**d**) large petaloid agranulocyte with densely stained nuclei; (**e**) roundish agranulocyte with densely stained nuclei; (**f**) granulocyte with weakly stained nuclei; (**g**) binucleated cell; and (**h**) fusiform cell. Values were obtained from three independent separations. Bar 5 μm. Source: Graphic by authors.

3.2.2. Functional Analysis

Functional analysis was performed for each gradient fraction in each of the 12 cell separation experiments.

The test revealed different behaviors of coelomocytes from Percoll density gradient fractions in vitro and from incubation in seawater. We used the term "behavior" for adhesive characteristics of cells, and both cell–cell and cell–substrate interactions. A typical picture of total coelomocyte suspension behavior is presented in Figure 2A(a): cells after 1.5 h of incubation in seawater formed the nets of cells. However, cells of fractions 1 and 2 did not form networks after 1.5 h (Figure 2A(b,c)) or after 18 h (Figure 2B(b,c)), while cells of fractions 4–5 formed networks after 1.5 h (Figure 2A(e,f)), and a clotting reaction occurred after 18 h (Figure 2B(e,f)). Cells of fraction 3 demonstrated an intermediate behavior (Figure 2A(d),B(d)).

These patterns of cell behavior in vitro were typical for cells of different fractions in about 90% of the experiments. In 1 experiment of the 12 carried out, the coelomocytes did not form networks in the total suspension or in the fractions. Circulatory coelomocytes were isolated from the starfish after 4 days of starvation in this case. The maximum number of cells was found in fraction 1 (Figure 2C). The composition of the total suspension of these coelomocytes significantly differed from that usually observed—the suspension was dominated by roundish (not petaloid) cells with fine-grained cytoplasm (Figure 2D), which in other experiments were observed mainly in fractions 1 and 2.

3.2.3. Separation of CE Cells in Percoll Density Gradients

A comparison of the proportion of cells in different CE fractions revealed the maximum proportion of cells in fractions 3 and 4 and the minimum in fraction 5 (Figure 3A), while for CE-W cells, these fluctuations were not so significant. The maximum variability for cell number was found for fractions 3 and 4 of the CE and fraction 4 of CE-W cells (Figure 3B).

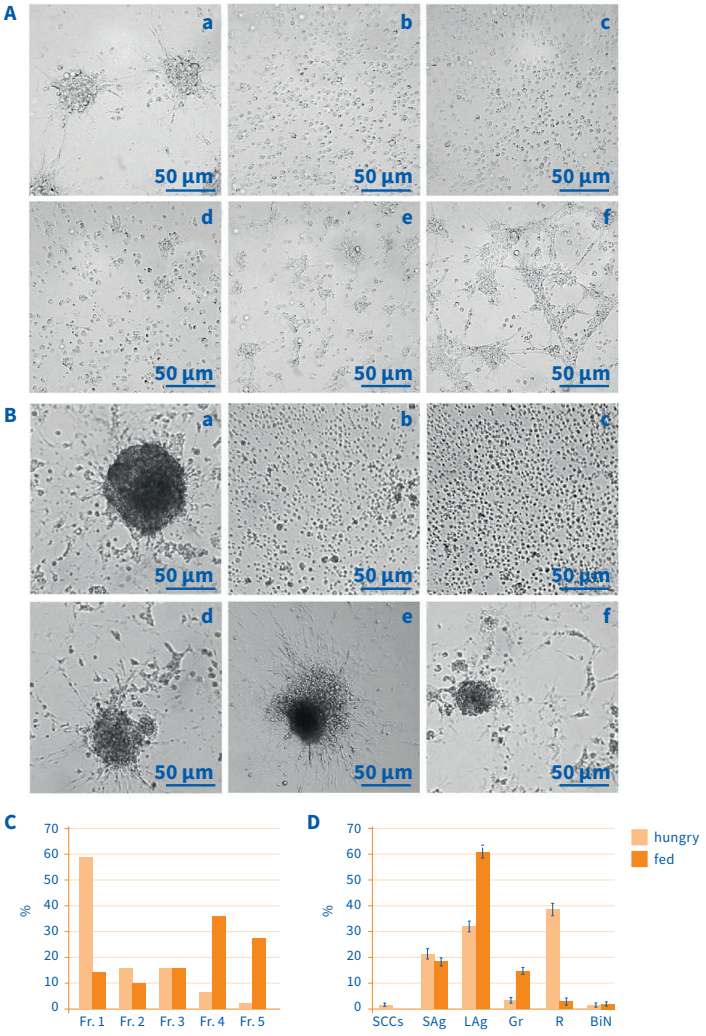

Figure 2. Functional test for Percoll-separated coelomocyte suspensions. (**A**) Behavior of coelomocytes of different fractions after 1.5 h cell incubation in seawater: (**a**) a typical picture of total cell suspension behavior, net formation; (**b**–**f**) behavior of coelomocytes from fractions 1–5. (**B**) Behavior of coelomocytes of different fractions after 18 h cell incubation in seawater: (**a**) clotting reaction of total cell suspensions; (**b**–**f**) behavior of coelomocytes from fractions 1–5. (**C**) Comparison of cell number in each fraction in hungry (white columns) and fed (gray columns) animals. (**D**) Comparison of the cell composition of total coelomocyte suspensions for hungry (white columns) and fed (gray columns) animals. SCCs—small coelomocytes; Sag—small agranulocytes; Lag—large agranulocytes; Gr—granulocytes; R—roundish coelomocytes; BiN—binucleated cells. Source: Graphic by authors.

3.2.4. The Composition of CE Cell Gradient Fractions

The cell types of the CE and of CE-W cells (epitheliocytes) are presented in Figure 3C. Analysis of images after staining with DAPI made it possible to subdivide small agranulocytes of the CE into two subtypes. Dominant cell types in the total CE cell suspension (Figure 3C(a)) were small agranulocytes with irregularly shaped nuclei (4.8 $\pm$ 0.17 μm), which tended to form aggregates. Only this type of agranulocyte was attributed to ciliated epithelial cells. Small agranulocytes with roundish nuclei (6 $\pm$ 0.33 μm) were assigned to a different type (Figure 3C(b)). Other cell types were as follows: two types of small cells with a high nuclear–cytoplasmic ratio: small epitheliocytes with discretely stained roundish (4.06 $\pm$ 0.2 μm) or oval (4 $\times$ 4.06 $\pm$ 0.5 μm) nuclei (Figure 3C(c)) and invisible cytoplasm (SECs-1) and small cells (3.3 $\pm$ 0.2 μm) with densely stained nuclei (SECs-2) (Figure 3C(d)); large agranulocytes with densely stained roundish nuclei (9.5 $\pm$ 0.33 μm) (Figure 3C(e)); large eosinophilic granulocytes with weakly stained nuclei and two or more eosinophilic granules in the cytoplasm (9.3 $\pm$ 0.5 μm) (Figure 3C(f)). Other cells identified in the CE previously included: small azurophilic granulocytes with densely stained nuclei, morula cells with weakly stained bean-shaped acentric nuclei, and enucleated cells varying in size (2–12 μm) and shape. These were not identified after DAPI staining. Therefore, they were not evaluated in these experiments.

Analysis of the composition of CE gradient fractions revealed the presence of ciliated cells in all fractions of the gradient (Figure 3C(a)). This is the dominant type of cell. In addition, small agranulocytes with roundish nuclei were found in the same fractions in a significant amount. Enrichment of fraction 1 with small cells of type 2 (SECs-2) was found. In addition, the smallest number of large eosinophilic granulocytes was found in fraction 1; their share increased in heavier fractions.

Separation of the subpopulation of CE-W cells, enriched with SECs-1, showed other traits (Figure 3C). SECs-1 were abundantly revealed in fractions 1–3 (Figure 3C(c)). Ciliated cells occupy a much smaller proportion in the total population of CE-W cells compared to the CE. Their share in fractions 1–3 is even lower. Enrichment of fractions 4–5 with small agranulocytes (Figure 3C(b)) and fraction 4 with large agranulocytes (Figure 3C,E) was revealed.

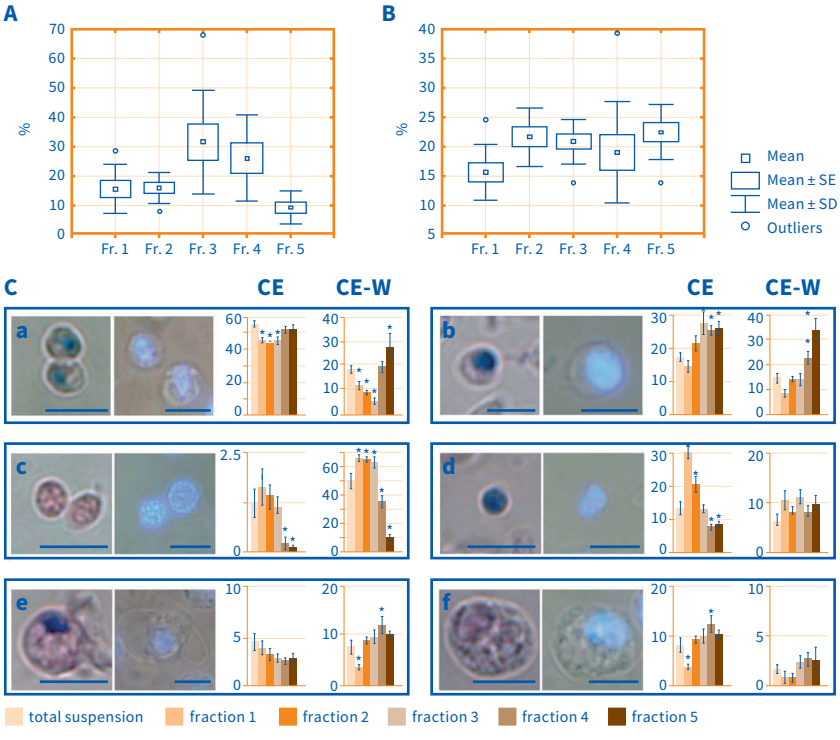

Figure 3. Coelomic epithelium (CE) and CE weakly bound (CE-W) cell separation in discontinuous Percoll density gradients. (**A**) The portion of cells in different fractions of the CE. (**B**) The portion of cells in different fractions of CE-W cells. (**C**) The epitheliocyte types revealed after azure-eosin staining and staining of cell suspensions with DAPI and the portion of this type in each gradient fraction of CE and CE-W cells: (**a**) small agranulocyte with irregularly shaped nuclei (ciliated cell); (**b**) small agranulocyte with roundish nuclei; (**c**) small epitheliocyte with discretely stained nuclei and invisible cytoplasm; (**d**) small epitheliocyte with densely stained nuclei and invisible cytoplasm; (**e**) large agranulocytes with densely stained roundish nuclei; and (**f**) large granulocytes with weakly stained nuclei and two or more granules in the cytoplasm. Bar 5 µm. Source: Graphic by authors.

3.2.5. Functional Test

Cells of different CE fractions exhibited different behavior when incubated in seawater (Figure 4A–F).

The peculiarities were revealed only after 18 h of incubation. Cells of fractions 1 and 2 remained solitary during the entire period of time, while cells of fractions 3–5 formed aggregates. The staining of the cells with anti-tubulin antibody and DAPI showed that these aggregates are composed of ciliated cells (Figure 4G).

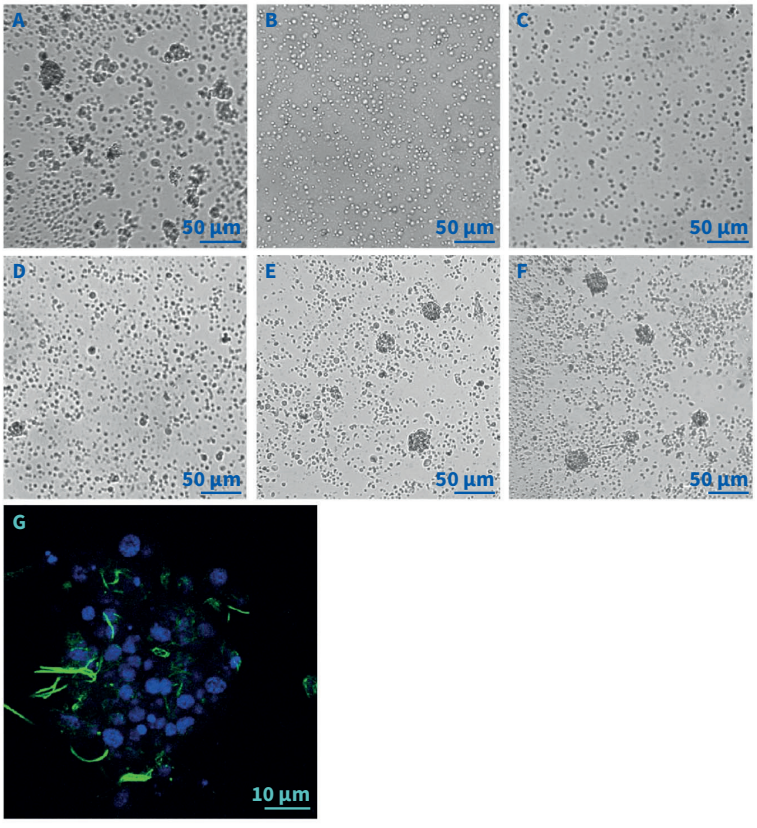

Figure 4. Functional test for Percoll-separated epitheliocyte suspensions after 18 h of cell incubation in seawater. (**A**) A typical picture of total cell suspension behavior, aggregate formation. (**B**–**F**) Behavior of epitheliocytes from fractions 1–5. (**G**) Aggregate of ciliated cells after the staining of the CE cells with anti-tubulin antibody (green) and DAPI (blue). Source: Graphic by authors.

4. Discussion

In this study, circulatory cells of the CF and cells of two subpopulations of the *A. rubens* CE were separated in Percoll density gradients, and the morphology and behavior of cells in each fraction of the gradient in vitro were characterized.

This study was undertaken with the aim of isolating subpopulations of cells enriched with certain morphotypes for subsequent proteomic analysis. The need for this is associated with the difficulties of assessing the origin of cells in heterogeneous populations based only on morphological data. The general problem can be formulated as follows: to find out whether coelomocytes are a single line of cells at different stages of differentiation, or whether there are distinct sources for different types of cells.

The literature provides examples of the separation of invertebrate cells in density gradients, followed by the characterization of the cytotoxicity and immune characteristics of the cells.

Separation of earthworm (*Eisenia foetida*) coelomocytes in Percoll density gradients revealed four fractions of cells. Four cell types that differ significantly morphologically and functionally (Kauschke et al. 2001; Hamed et al. 2005) were classified in them: acidophils, basophils, chloragocytes, and neutrophils. The second fraction was composed mainly of basophils (40%), and the fourth fraction was enriched with basophils (60%) and neutrophils (35%). Basophils and neutrophils showed the greatest cytotoxic activity against the human immortalized myelogenous leukemia cell line K562 (Kauschke et al. 2001).

Separation of coelomocytes of purple sea urchins, *Arbacia punctulata*, in Percoll density gradients led to isolation of four cell types: white cells, which are called phagocytic amebocytes (>99.5% pure), vibratile cells (>93% pure), granular white spherule cells (white morula cells), and red spherule cells (red morula cells, >99% pure) (Lin et al. 2001). White phagocytic amebocytes showed the greatest cytotoxic activity against human K562 target cells compared to total coelomocytes.

Separation of the blood cells of *Styela rustica* (Styelidae, Stolidobranchiae) in discontinuous Percoll gradients led to more than 90% enrichment with morula cells of the bottom fraction (Podgornaya and Shaposhnikova 1998).

Coelomocytes of *Asterias rubens* were firstly separated in a four-step discontinuous density gradient of sodium diatrizoate (Kudryavtsev et al. 2016). Three cell fractions were obtained after centrifugation of circulatory coelomocytes. Small cells (lymphocyte-like agranulocytes) with a high nuclear–cytoplasmic ratio predominated in the upper fraction ($\geq$95%). These cells expressed a homolog of the C3 gene, a component of the complement system, in response to stimulation with bacterial lipopolysaccharides. Cells with small granules evenly distributed in the cytoplasm were typical for the middle fraction (73%–80%). They demonstrated an ability to produce reactive oxygen species and phagocytosis. The cells of the lower fraction, large coelomocytes with a high content of large granules and vesicles in the perinuclear space (75%–85%), had a high level of hemolytic activity and neutral red uptake.

Centrifugation of coelomocytes and CE cells in a six-step Percoll density gradient, undertaken in the present study, resulted in the appearance of six zones of cells formed at the boundaries of the steps. Cells were mainly redistributed among fractions 1–5. The sixth fraction (55% Percoll) contained an insignificant proportion of cells, mostly destroyed, and was excluded from consideration.

In this study, we identified eight conditional morphotypes of coelomocytes after staining with azure-eosin and DAPI, in contrast to the three types proposed by Kudryavtsev et al. (2016). This led to a more complex picture when characterizing the

composition of the fractions. Compared to our previous classification, we identified and isolated another type of CF cells, roundish agranulocytes, which were rarely represented in the total population and previously referred to as agranulocytes. Moreover, DAPI staining revealed a new cell type among the CE cell population, small agranulocytes with roundish nuclei. Roundish coelomocytes and small agranulocytes of the CE with a roundish nucleus are probably independent types of cells of the CF and CE, respectively.

Analysis of the composition of fractions revealed significant enrichment of fractions 1 and 2 with roundish (not petaloid) cells. Their share in the total suspension of coelomocytes was very small. Granules were not detected in the cytoplasm of these cells after staining with azure-eosin. They did not form networks and did not show a clotting reaction in the functional test. Therefore, these cells can be considered separate from petaloid agranulocytes. They could be isolated with an enrichment of 58% in fraction 1 and 40% in fraction 2. Fractions 4–5 were enriched (55% and 40%, respectively) in petaloid agranulocytes, which showed network formation and clotting response in the functional test.

The stability of the results of the functional test was disturbed in only 1 case out of 12, when the cells did not even form networks in the total coelomocyte suspension or in fraction 4. In this case, the total cell population contained 40% of roundish cells, the maximum number of cells was detected in fraction 1, and the proportion of petaloid cells was 30% compared to 50% in other cases. This fact correlated with the 4-day starvation of the animals. A previous study showed the importance of such a physiological parameter as "fed-hungry" for the coelomocyte concentration: starvation leads to a decrease in the concentration of circulating coelomocytes, while feeding leads to an increase in this value (Sharlaimova et al. 2020). The fact of the relationship between starvation and the composition of circulating coelomocytes needs to be confirmed by further research.

The less represented types of cells, small cells with a high nuclear–cytoplasmic ratio, granulocytes, and binucleated cells, also demonstrated enrichment in distinct gradient fractions. However, their number was insufficient for subsequent proteomic analysis. Other approaches are required to isolate these cell morphotypes.

Separation of CE cells in a Percoll density gradient revealed ciliated cells in all fractions of the gradient. However, the functional test exhibited unequal behavior of ciliated cells of different fractions: cells of fractions 1 and 2 remained singular during the entire observation period, and cells of fractions 4 and 5 formed cell aggregates. This indicates the heterogeneity of the buoyant density of ciliated cells, which can be explained by the presence of several types of epithelia in the CE: a flat epithelium on the mesentery, and a cuboid or cylindrical epithelium in other regions of the CE (Sharlaimova et al. 2020).

The more interesting result in the case of CE cell separation is the enrichment in fraction 1 with SECs-2. These cells are the second type of small proliferating cells of the CE with unknown functions, identified both in the cellular suspension and with electron microscopy (Sharlaimova et al. 2014).

The total suspension of the subpopulation of CE-W cells was enriched in SECs-1 cells, proposed to be the progenitor for some coelomocytes. This fact made it possible to identify proteins that can serve as markers of these cells (Sharlaimova et al. 2020). Gradient fractionation further increases the proportion of SECs-1 in the suspension. SECs-1 were distributed among fractions 1–3, that is, in three Percoll densities, which confirms the heterogeneity of the population of these cells. Earlier, the assumption about their heterogeneity was made on the basis of electron microscopic studies (Sharlaimova et al. 2020). Separation of CE-W cells also makes it possible to obtain enrichment with small agranulocytes with roundish nuclei and ciliated epithelial cells in fraction 5, in which the share of SECs-1 and SECs-2 is insignificant. The position and function of small agranulocytes with roundish nuclei, cells that we separated into an independent morphotype based on image analysis after cell staining with DAPI in this study, are unclear.

5. Conclusions

Separation of the coelomic fluid and coelomic epithelial cells in Percoll density gradients made it possible to isolate several enriched morphotypes of cells from heterogeneous populations. For cells of the coelomic fluid, these were roundish agranulocytes and petaloid agranulocytes, presumably two stages of coelomocyte differentiation. Separation of the coelomic epithelium allowed the isolation of small epithelial type 2 cells and ciliated cells, characterized by the ability to form aggregates in vitro. Separation of CE-W cells primarily permitted the isolation of small epithelial type 1 cells, which are proposed progenitors for some types of coelomocytes, and small agranulocytes with roundish nuclei, which are cells with unclear functions. This study creates the basis for proteomic analysis of cell fractions enriched with a certain morphotype.

Identification of surface and membrane protein markers of poorly differentiated cells of the coelomic epithelium, as well as protein markers of specialized cells of the coelomic fluid and coelomic epithelium, allows tracking the differentiation or dedifferentiation of cells. The results of this study contribute to the elucidation of the mechanisms of coelomocyte replenishment.

Author Contributions: Designed the study: O.P.; conducted the experiments and processed the data: O.P., S.S., N.S., and D.B.; prepared the figures: N.S.; writing—original draft preparation, O.P.; discussion and editing: N.S. and O.P. All authors have read and agreed to the published version of the manuscript.

Funding: This research was carried out within the state assignment of the Ministry of Science and Higher Education of the Russian Federation (No. AAAA-A19-119020190093-9) and was funded by the Director's Fund of the Institute of Cytology of the Russian Academy of Sciences.

Acknowledgments: We are grateful to the administration and staff of the White Sea Biological Station "Kartesh" of the Zoological Institute, Russian Academy of Sciences, for providing the conditions for the work and very valuable assistance.

Conflicts of Interest: The authors declare no conflict of interest.

Abbreviations

CE	Coelomic epithelium
CE-W	Subpopulation of weakly attached CE cells
CF	Coelomic fluid
SECs-1	Small epithelial cells of type 1
SECs-2	Small epithelial cells of type 2

References

Blanpain, Cédric, and Elaine Fuchs. 2014. Plasticity of epithelial stem cells in tissue regeneration. *Science* 344: 1242281. [CrossRef]

Blowes, Liisa M., Michaela Egertová, Yankai Liu, Graham R. Davis, Nick J. Terrill, Himadri S. Gupta, and Maurice R. Elphick. 2017. Body wall structure in the starfish *Asterias rubens*. *Journal of anatomy* 231: 325–41. [CrossRef] [PubMed]

Bosch, Thomas C.G. 2009. Hydra and the evolution of stem cells. *BioEssays* 31: 478–86. [CrossRef] [PubMed]

Bossche, J.-P. Vanden, and Michel Jangoux. 1976. Epithelial origin of starfish coelomocytes. *Nature* 261: 227–28. [CrossRef] [PubMed]

Chia, Fu-Sh, and Jun Xing. 1996. Echinoderm Coelomocytes. *Zoological Studies-Taipei-* 35: 231–54.

De Mulder, Katrien, Georg Kuales, Daniela Pfister, Maxime Willems, Bernhard Egger, Willi Salvenmoser, Marlene Thaler, Anne-Kathrin Gorny, Martina Hrouda, Gaëtan Borgonie, and et al. 2009. Characterization of the stem cell system of the acoel *Isodiametra pulchra*. *BMC Developmental Biology* 9: 69. [CrossRef] [PubMed]

Dogel, Valentine A. 1981. *Zoology of Invertebrates*, 7th ed. Moscow: Higher School, p. 606. (In Russian)

Ferrario, Cinzia, Michela Sugni, Ildiko M. L. Somorjai, and Loriano Ballarin. 2020. Beyond Adult Stem Cells: Dedifferentiation as a Unifying Mechanism Underlying Regeneration in Invertebrate Deuterostomes. *Frontiers in Cell and Developmental Biology* 8: 587320. [CrossRef]

Funayama, Noriko. 2018. The cellular and molecular bases of the sponge stem cell systems underlying reproduction, homeostasis and regeneration. *The International Journal of Developmental Biology* 62: 513–25. [CrossRef]

García-Arrarás, José E., and Igor Yu Dolmatov. 2010. Echinoderms: Potential Model Systems for Studies on Muscle Regeneration. *Current Pharmaceutical Design* 16: 942–55. [CrossRef]

Hamed, Sherifa S., E. Kauschke, and E. L. Cooper. 2005. Cytochemical properties of earthworm coelomocytes enriched by percoll. *International Journal of Zoological Research* 1: 74–83. [CrossRef]

Kanungo, Kalpataru T. 1982. In vitro studies on the effect of cell–free coelomic fluid, calcium, and/or magnesium on clumping of coelomocytes of the sea star *Asterias forbesi* (Echinodermata: Asteroidea). *The Biological Bulletin* 163: 438–52. [CrossRef]

Kassmer, Susannah H., Adam D. Langenbacher, and Anthony W. De Tomaso. 2020. Integrin alpha-6+ candidate stem cells are responsible for whole body regeneration in the invertebrate chordate *Botrylloides diegensis*. *Nature communications* 11: e4435. [CrossRef] [PubMed]

Kauschke, Ellen, Kazuo Komiyama, Itaru Moro, Ines Eue, Simone König, and Edwin L. Cooper. 2001. Evidence for perforin-like activity associated with earthworm leukocytes. *Zoology* 104: 13–24. [CrossRef] [PubMed]

Kudryavtsev, Igor V., Ivan S. D'yachkov, Denis A. Mogilenko, Alexander N. Sukhachev, and Alexander V. Polevshchikov. 2016. The Functional Activity of Fractions of Coelomocytes of the Starfish *Asterias rubens* Linnaeus, 1758. *Russian Journal of Marine Biology* 42: 158–65. [CrossRef]

Lin, Wenyu, Haiyan Zhang, and Gregory Beck. 2001. Phylogeny of Natural Cytotoxicity: Cytotoxic Activity of Coelomocytes of the Purple Sea Urchin, *Arbacia punctulata*. *Journal of Experimental Zoology* 290: 741–50. [CrossRef] [PubMed]

Pellettieri, Jason, and Alejandro Sánchez Alvarado. 2007. Cell Turnover and Adult Tissue Homeostasis: From Humans to Planarians. *Annual Review of Genetics* 41: 83–105. [CrossRef]

Podgornaya, Olga I., and Tatjana G. Shaposhnikova. 1998. Antibodies with the Cell-type Specificity to the Morula Cells of the Solitary Ascidians *Styela Rustica* and *Boltenia Echinata*. *Cell structure and Function* 23: 349–55. [CrossRef]

Rinkevich, Baruch, Loriano Ballarin, Pedro Martinez, Ildiko Somorjai, Oshrat Ben-Hamo, Ilya Borisenko, Eugene Berezikov, Alexander Ereskovsky, Eve Gazave, Denis Khnykin, and et al. 2022. A pan-metazoan concept for adult stem cells: The wobbling Penrose landscape. *Biological Reviews* 97: 299–325. [CrossRef]

Rossi, Leonardo, and Alessandra Salvetti. 2019. Planarian stem cell niche, the challenge for understanding tissue regeneration. *Seminars in Cell & Developmental Biology* 87: 30–36. [CrossRef]

Sharlaimova, Natalia, Sergey Shabelnikov, and Olga Petukhova. 2014. Small coelomic epithelial cells of the starfish *Asterias rubens* L. that are able to proliferate in vivo and in vitro. *Cell and Tissue Research* 356: 83–95. [CrossRef]

Sharlaimova, Natalia, Sergey Shabelnikov, Dan Bobkov, Marina Martynova, Olga Bystrova, and Olga Petukhova. 2020. Coelomocyte replenishment in adult *Asterias rubens*: The possible ways. *Cell and Tissue Research* 383: 1043–60. [CrossRef] [PubMed]

Sharlaimova, N.S., and O.A. Petukhova. 2012. Characteristics of populations of the coelomic fluid and coelomic epithelium cells from the starfish *Asterias rubens* L. able attach to and spread on various substrates. *Cell and Tissue Biology* 6: 176–88. [CrossRef]

Simpson, Tracy L. 1984. *The Cell Biology of Sponges*. New York: Springer, p. 662. [CrossRef]

Smith, Valerie J. 1981. The echinoderms. In *Invertebrate Blood Cells*. Edited by Norman A. Ratcliffe and Andrew F. Rowley. London: Academic Press, pp. 513–62.

Sugio, Mutsumi, Chikako Yoshida-Noro, Kaname Ozawa, and Shin Tochinai. 2012. Stem cells in asexual reproduction of Enchytraeus japonensis (Oligochaeta, Annelid): Proliferation and migration of neoblasts. *Development, Growth & Differentiation* 54: 439–50. [CrossRef]